JOURNAL OF GEOPHYSICAL RESEARCH, VOL. 91, NO. D11, PAGES 11,851–11,866, OCTOBER 20, 1986

Approximate Methods for Finding CO_2 15-μm Band Transmission in Planetary Atmospheres

DAVID CRISP[1]

Geophysical Fluid Dynamics Program, Princeton University, Princeton, New Jersey

STEPHEN B. FELS AND M. D. SCHWARZKOPF

Geophysical Fluid Dynamics Laboratory, National Oceanic and Atmospheric Administration Princeton University, Princeton, New Jersey

The CO_2 15-μm band provides an important source of thermal opacity in the atmospheres of Venus, Earth, and Mars. Efficient and accurate methods for finding the transmission in this band are therefore needed before complete, self-consistent physical models of these atmospheres can be developed. In this paper we describe a hierarchy of such methods. The most versatile and accurate of these is an "exact" line-by-line model (Fels and Schwarzkopf, 1981). Other methods described here employ simplifying assumptions about the structure of the 15-μm band which significantly improve their efficiency. Because such approximations can reduce the accuracy of a model, as well as its computational expense, we established the range of validity of these simpler models by comparing their results to those generated by the line-by-line model. Pressures and absorber amounts like those encountered in the atmospheres of Venus, Earth, and Mars were used in these tests. Physical band models based on the Goody (1952) random model compose the first class of approximate methods. These narrow-band models include a general random model and other more efficient techniques that employ the Malkmus (1967) line-strength distribution. Two simple strategies for including Voigt and Doppler line-shape effects are tested. We show that the accuracy of these models at low pressures is very sensitive to the line-strength distribution as well as the line shape. The second class of approximate methods is represented by an exponential wideband model. This physical band model is much more efficient than those described above, since it can be used to find transmission functions for broad sections of the CO_2 15-μm band in a single step. When combined with a simple Voigt parameterization, this method produces results almost as accurate as those obtained from the more expensive narrow-band random models. The final class of approximate methods tested here includes the empirical logarithmic wideband models that have been used extensively in climate-modeling studies (Kiehl and Ramanathan, 1983; Pollack et al., 1981). These methods are very efficient, but their range of validity is more limited than that of the other methods tested here. These methods should therefore be used with caution.

1. INTRODUCTION

Absorption and emission within the CO_2 15-μm band provide an important source of thermal radiative cooling in the atmospheres of Venus, Earth, and Mars. Complete, self-consistent numerical models of the thermal structures and dynamical states of these atmospheres therefore require reliable descriptions of the transmission within this band. The most versatile and accurate methods for finding this transmission are the line-by-line models, such as those described by *Drayson* [1967] and *Fels and Schwarzkopf* [1981]. These methods are called "exact," since they can employ all available information about absorption lines shapes, strengths, and positions, and their accuracy is limited primarily by uncertainties in these line parameters. Unfortunately, the complexity and computational expense of these methods makes them impractical for use in many climate-modeling problems where thermal infrared optical properties are not well established or where the band transmittance must be computed often. Two such problems are encountered in studies of the Martian atmosphere. In the Martian atmosphere the total atmospheric mass changes significantly during the annual cycle and the atmospheric opacity and temperature structure can change dramatically at some altitudes during global dust storms. In the Venus atmosphere the CO_2 mixing ratios are well known, but uncertainties in the concentrations of other thermal opacity sources (H_2O, SO_2, H_2SO_4) jeopardizes the accuracy achieved with the CO_2 line-by-line calculation. Expensive line-by-line methods are also impractical for investigations of the primitive terrestrial atmosphere, where CO_2 mixing ratios are not well known, or in studies of the transient response of the present atmosphere to increasing CO_2 amounts. For such problems, more efficient approximate methods are needed.

In this paper we describe a hierarchy of physical band models that employ simplifying assumptions about the structure of the CO_2 15-μm band. Because such simplifications can reduce the accuracy and range of validity of a model as well as its computational expense, each approximate method was tested by comparing its results to those obtained from the *Fels and Schwarzkopf* [1981] line-by-line model. In addition to these physical band models we tested two empirical absorption correlation functions that model the curve of growth of the CO_2 15-μm band. Our model atmospheres include pressures, temperatures, and CO_2 amounts like those that occur along optical paths in the atmospheres of Venus, Earth, and Mars. These model atmospheres have CO_2 mass mixing ratios of 0.0005 and 1.0, at pressures between 10^{-6} and 1 atm. We show that if 10% errors in the absorption and 20% errors in cooling rates for the 15-μm band are acceptable, methods that are vastly more efficient than the line-by-line model can be used for the entire range of pressures and CO_2 path lengths described above. Such methods may provide both the economy and accuracy needed in climate-modeling problems where line-by-line methods are not practical.

[1]Now at Division of Geological and Planetary Sciences, California Institute of Technology, Pasadena.

Paper number 6D0395.
0148-0227/86/006D-0395$05.00

TABLE 1. Precis of Parameterized Models

	$\Delta\nu$, cm^{-1}	Line Shape	Line Intensity Distribution, $P(S)$	Lorentz-Voigt-Doppler Transition	Comparison with Line-by-Line Model
			Narrow-Band Models		
General random	5	rectangular core; ν^{-2} wings [*Fels*, 1979]	true distribution for each interval	automatic	Figures 6 and 7
Lorentz-Malkmus	5	Lorentz	$N S^{-1} \exp(-S/k)$ [*Malkmus*, 1967]	Lorentz only	Figures 8 and 9
Fels-Malkmus	5	[*Fels*, 1979]	[*Malkmus*, 1967]	automatic	Figures 10 and 11
Doppler general random	50	rectangular	true distribution	Doppler only	...
Lorentz-Malkmus with Doppler correction	hybrid	Lorentz and Doppler	hybrid	*Rodgers and Williams* [1974] used to join Lorentz-Malkmus and Doppler general random model results	Figures 12 and 13
			Broadband Models		
Exponential wideband	~200	Lorentz	Integral over many narrow intervals with *Malkmus* [1967] distributions [*Wang*, 1983]	Lorentz only	...
Wideband Doppler model	~200	rectangular	$Nk^{-1} S^{-5/4} \exp(-S/k) + lS^{-5/4} \exp(-S/\psi)$	Doppler only	...
Exponential wideband with Doppler correction	hybrid	Lorentz and Doppler	hybrid	*Rodgers and Williams* [1974] used to join Lorentz exponential wideband and wideband Doppler model results	Figures 14 and 15
Kiehl and Ramanathan	350	...	...	...	Figures 16 and 17
Pollack et al.	~450	...	...	...	Figures 18 and 19

2. DESCRIPTION OF MODELS

The methods developed here can be classified as "narrow-band" or "broadband" techniques. For example, the line-by-line model can be considered the ultimate narrow-band method, since the spectral region occupied by the CO_2 15-μm band must be divided into intervals small enough that even the narrow Doppler cores of individual lines are completely resolved. The broadband transmittance is obtained from these models by first finding the transmission in each narrow interval and then integrating these results numerically over the desired spectral region.

The first class of approximate methods considered are the "random" models, such as those described by *Goody* [1952, 1964], *Malkmus* [1967], and *Fels* [1979]. These are also narrow-band models, since they must be applied to relatively narrow fractions of a band if accurate results are needed. Narrow spectral intervals must be used with these models, since the effects of overlap between spectral lines is accounted for by assuming that the lines are positioned randomly throughout the chosen spectral interval. If such models are applied to the entire CO_2 15-μm band (450–870 cm^{-1}), the large number of strong lines clustered near the center of the band (650–680 cm^{-1}) are assumed to be scattered randomly throughout this spectral region. For this extreme case the amount of overlap between these lines will be seriously underestimated. This problem can be avoided if the band is divided into spectral intervals small enough so that the mean strength and spacing of absorption lines does not vary significantly across each. For the CO_2 15-μm band this criterion is met if spectral intervals no wider than about 5 cm^{-1} are used [*Kiehl and Ramanathan*, 1983].

In sections 2.2, 2.3, and 2.6, four narrow-band random models are described. The first is a "general" random model [*Goody*, 1964]. This model employs an accurate description of the line-strength distribution within the 15-μm band and a simplified Voigt line shape [*Fels*, 1979]. The second model is the one described by *Malkmus* [1967] and *Rodgers* [1968], which assumes an S^{-1} tailed line-intensity distribution and a Lorentz line shape. The third random model also employs the Malkmus line-strength distribution, but it uses the *Fels* [1979] simplified Voigt line shape, rather than the Lorentz profile. The last narrow-band method is described in section 2.6. This is a hybrid method that incorporates a Malkmus random model for Lorentz lines and a simplified general random model for Doppler lines. The empirical interpolation formula given by *Rodgers and Williams* [1974] is used to combine the results of these two models. The accuracy of these methods is demonstrated in section 3.3.

Three broadband models are described in sections 2 and 3. The first is related to the "exponential wide-band" models developed by *Edwards and Menard* [1964*a*, *b*], *Edwards and Balakrishnan* [1973], *Kuo* [1977], and *Wang* [1983]. These models avoid the numerical integration over frequency required by the above random models by assuming that the mean line strength decreases exponentially with increasing dis-

tance from the band center. *Wang* [1983] shows that when this parameterization is combined with assumptions of random line spacing and the Malkmus line-strength distribution, the transmission function for an entire band, or broad sections of it, assumes a simple functional form. In section 2.4 we describe a new exponential wideband model of the CO_2 15-μm band. A simple method for incorporating Voigt lineshape effects into such broadband models is described in section 2.6. In section 3.4 we show that in spite of this model's efficiency, its accuracy and range of validity are comparable to that of the more expensive narrow-band random models. The two other broadband models described here are empirical absorptance correlation functions [*Kiehl and Ramanathan* [1983] and *Pollack et al.* [1981]. These methods are designed to model the curve of growth instead of the structure of the CO_2 15-μm band. The performance of these methods is illustrated in section 3.5. The important features of the various narrow-band and broadband models are summarized in Table 1.

2.1. *The Line-by-Line Model*

Because a complete description of the present line-by-line model has been published elsewhere [*Drayson*, 1967; *Fels and Schwarzkopf*, 1981], only a brief review of its features will be outlined here. A few important differences in its use will also be noted. The transmission in a wave number interval $\Delta\nu$ between pressure levels p and p' in a plane-parallel hydrostatic atmosphere is given by

$$\tau(p, p') = \frac{1}{\Delta\nu}\int_{\Delta\nu} d\nu \exp\left\{-\frac{1}{\mu g}\int_p^{p'} r\, dp''\left[\sum_{i=1}^{N} k_i(\nu, p'', T)\right]\right\} \tag{1}$$

where T is temperature, ν is wave number, μ is the cosine of the zenith angle, g is the gravitational acceleration, r is the CO_2 mass mixing ratio, k_i is the monochromatic absorption coefficient due to the ith line, and N is the total number of lines contributing to absorption at this wave number.

In a line-by-line model the integrals over wave number and pressure are evaluated numerically. The details of these integration schemes are described by Drayson and Fels and Schwarzkopf. The principal advantage of this method is that all of the available information about the line strengths, shapes, and positions, as well as variations in the first two of these quantities which occur along atmospheric optical paths, can be incorporated into the transmittance calculation. These methods can therefore produce accurate results in the spectral region occupied by the CO_2 15-μm band, since the line parameters there are relatively well known.

We used the line-by-line model to find the transmittance in nine 50 cm^{-1} wide spectral intervals in the region extending from 450 to 900 cm^{-1}. This spectral domain contains almost the entire 15-μm band as well as a small piece of the 10.4-μm doubly hot band. We obtained the absorption line positions, widths, and strengths from the 1978 version of the Air Force Geophysical Laboratory (AFGL) catalog of line parameters [*Rothman and Benedict*, 1978]. (This newer AFGL catalogue includes very few changes for the CO_2 15-μm band.) Unlike in the work by *Fels and Schwarzkopf* [1981], here we used all 18,677 lines listed in this interval. This fact is important, since we will show that even the very weak lines can contribute significantly to the absorption along paths at low pressures. A Voigt line shape [*Hui et al.*, 1977] is used at pressures less than 0.1 atm. The sub-Lorentzian behavior of CO_2 line wings was parameterized by assuming that absorption by a given line ceased at a distance of 3 cm^{-1} from the line center [*Fels and Schwarzkopf*, 1981]. We found that for optical paths with mean pressures less than 1 atm, the total absorption in the 15-μm band varied by less than 1% when this cutoff was changed from 3 to 6 cm^{-1}. This suggests that our results are not sensitive to this approximation.

As we noted above, the principal shortcoming of the line-by-line model is its computational expense. Most of this expense results because the CO_2 15-μm band must be divided into wave number intervals small enough so that even the narrow cores of individual spectral lines can be adequately resolved, and the transmission must be evaluated in each of these intervals. Within the 15-μm band there are thousands of these intervals, some of which are less than 10^{-4} cm^{-1} wide. One can therefore achieve a tremendous improvement in efficiency if some aspect of the band structure can be parameterized in a way that allows the number of spectral interval divisions to be reduced significantly. Models that exploit such parameterizations are described in the following sections.

2.2 *The General Random Model for Simplified Voigt Lines*

If absorption lines are positioned randomly within a spectral interval of width $\Delta\nu$, where $\Delta\nu$ is much wider than the line half-width, the transmission function (1) can be simplified [*Goody*, 1964] to give

$$\tau(p, p') = \left\{1 - \left[\sum_{i=1}^{N} w_i(S, p, T)/(N\,\Delta\nu)\right]\right\}^N \tag{2}$$

where N is the total number of absorption lines within the interval and w_i is the equivalent width of the ith line, defined by

$$w_i(S, p, T) = \int_{-\infty}^{\infty} \{1 - \exp\left[-S_i(T) f_i(p, T, \nu)\bar{m}\right]\}\, d\nu \tag{3}$$

In this expression, $\bar{m}$ is the path-length-integrated absorber amount,

$$\bar{m} = \frac{1}{\mu}\int_p^{p'} \frac{r}{g}\, dp'' \tag{4}$$

T is temperature, μ is the cosine of the zenith angle, and the quantities S_i and f_i are the mean values of the line-strength and line-shape function, respectively, for the ith line along this path between pressures p and p'. If the spectral interval contains many lines (more than $\cong 10$), (2) can be simplified to

$$\tau(p, p') = \exp\left\{-\sum_{i=1}^{N} w_i(S, p, T)\Big/\Delta\nu\right\} \tag{5}$$

Equation (3) or (5) can be evaluated once the line-shape function f_i is defined. Because we are interested in obtaining transmittances for a very broad range of pressures (10^{-6} to 1 atm), the approximate Voigt line shape suggested by *Fels* [1979] was chosen. This function, shown in Figure 1, parameterizes a Voigt line as a rectangular "Doppler" core with Lorentzian wings:

$$\begin{aligned} f_i(\nu) &= C_i & |\nu| &\le \nu_0 \\ f_i(\nu) &= \alpha_L/\pi\nu^2 & |\nu| &> \nu_0 \end{aligned} \tag{6}$$

where ν is the distance from the line center, α_L is the Lorentz half-width at half-maximum, and

$$\nu_0 = (2/\pi)[1 + \zeta]\alpha_L + \beta\alpha_D \tag{7}$$

is the half-width of the rectangular line core. The constants, ζ and β, were chosen to give the proper equivalent widths in the

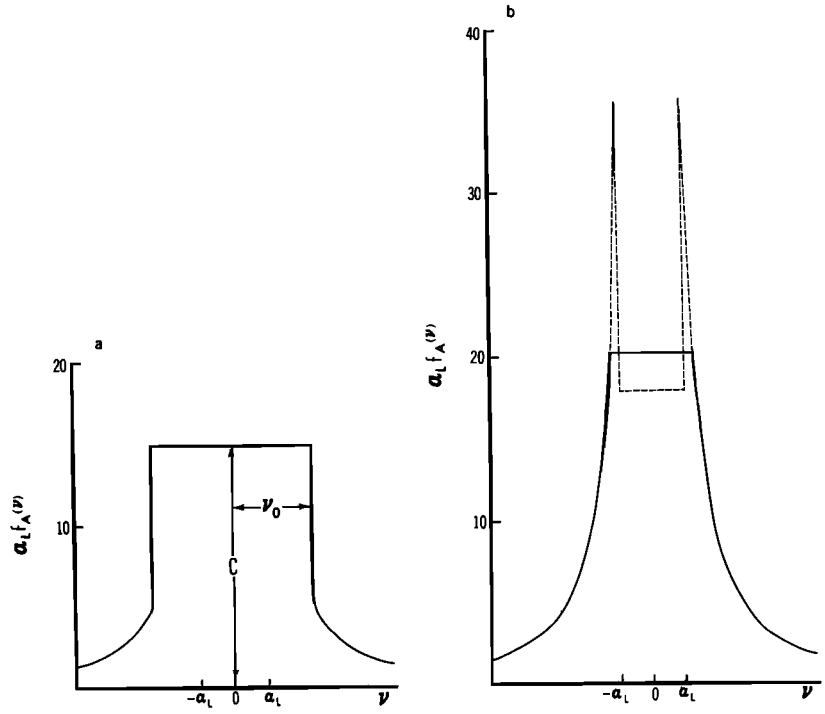

Fig. 1. The approximate Voigt line-shape function proposed by *Fels* [1979]. This function parameterizes a Voigt line as a rectangular "Doppler" core with Lorentz wings. (*a*) Line shape for $\alpha_L = \alpha_D$, $\beta = 1.25$, and $\zeta = 1$. (*b*) Line shape for pure Lorentz case ($\beta = 0$). The solid line is for $\zeta = 1$ and the dotted line is for $\zeta = 0.25$. (Reproduced from *Fels* [1979]).

Doppler and Lorentz limits. We found that $\zeta = 1.0$ and $\beta = 1.25$ gave acceptable results for the entire range of CO_2 mixing ratios used here. (For the terrestrial CO_2 mixing ratio, $\beta = 1.80$ produces somewhat more accurate results, while in pure CO_2 atmospheres, $\beta = 1.0$ is the best choice.) The Doppler half-width α_D is given by

$$\alpha_D = \bar{\nu} c^{-1} (2RT)^{1/2} \tag{8}$$

where $\bar{\nu}$ is the mean wave number in the spectral interval $\Delta\nu$, R is the gas constant for CO_2, and c is the speed of light. The constant C_i in (6), is the height of the rectangular line core. The value of this constant is constrained by the normalization condition:

$$\int_{-\infty}^{\infty} f(v)\, dv = 1$$

and is given by

$$C = (2\nu_0)^{-1} - \alpha_L (\pi \nu_0^2)^{-1} \tag{9}$$

When (6) is incorporated into (3), the resulting expression can be integrated to give

$$w_i(S, p, T) = 2\nu_0[1 - \exp(-S\bar{m}C_i)] + 2y\{\pi^{1/2} \operatorname{erf}(y/\nu_0) - \nu_0[1 - \exp(-(y/\nu_0)^2)]/y\} \tag{10}$$

where

$$y = [S\bar{m}\alpha_L/\pi]^{1/2}$$

and

$$\operatorname{erf}(y) = \frac{2}{\pi^{1/2}} \int_0^y \exp(-t^2)\, dt$$

is the error function.

Because (10) must be evaluated for each line in the spectral interval $\Delta\nu$, this band model is computationally expensive in spectral regions occupied by many lines. Fortunately, its efficiency can be improved significantly without producing a corresponding decrease in accuracy, if lines with similar strengths are gathered into line groups. Equation (10) can then be evaluated only once for each line group, and the transmission function becomes

$$\tau(p, p') = \left\{1 - \left[\sum_{j=1}^{J} n_j w_j \Big/ (N\,\Delta\nu)\right]\right\}^N \qquad N < 10$$
$$\tau(p, p') = \left[\exp\left(-\sum_{j=1}^{J} n_j w_j \Big/ \Delta\nu\right)\right] \qquad N \geq 10 \tag{11}$$

Here n_j is the number of lines in the jth group, J is the number of line groups, and w_j is the equivalent width (equation (10)), corresponding to the mean line strength and line width of the jth group.

We assume that a given line group contains only those lines with strengths that differ from the mean group line strength by less than 20%. This grouping criterion adds little real error to this model, since the line strengths used here are probably uncertain by 5–15% [*Fels and Schwarzkopf*, 1981]. Even when these narrow line groups are used, we find that this simplification reduces the computational expense of the general random model by factors of 5 to 25 in most spectral intervals.

The spectral interval width $\Delta\nu$ was limited to 5 cm^{-1} in these calculations, so that the distributions of strengths, widths, and spacings of absorption lines did not vary significantly across each interval. The line parameters S_i and α_{Li} in each interval were obtained form the 1978 version of the AFGL line-parameter compilation. (A listing of these line parameters can be obtained from the authors.) Variations in these quantities, which result from changes in pressure and temperature along realistic atmospheric optical paths, were parameterized by the Curtis-Godson approximation [*Rodgers and Walshaw*, 1966].

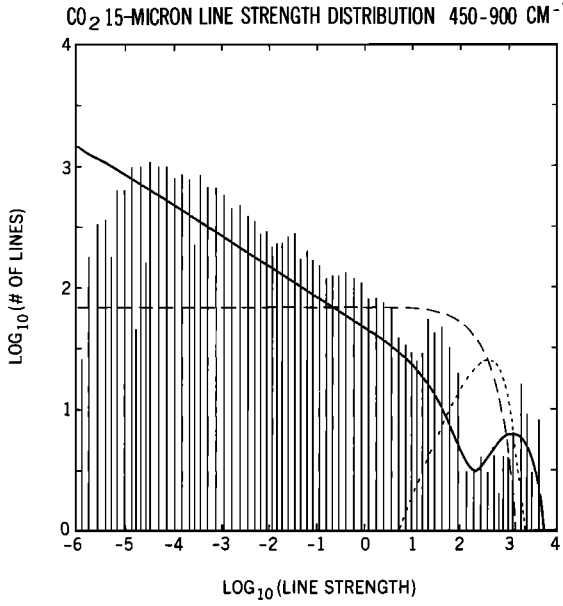

Fig. 2. A histogram (vertical bars) of all CO_2 lines on the AFGL line catalog at wave numbers between 450 and 900 cm^{-1}. Each bar represents the number of lines in a given line group. Lines with strengths within $\pm 20\%$ of the mean strength of a given group are gathered into that group. Analytic line-strength distributions obtained with the Goody (dotted line) and Malkmus (long-dashed line) models are also shown, along with the analytic distribution adopted for the wideband Doppler model (thin solid line) described in section 2.5.

2.3. *Random Models That Use the Malkmus Line-Strength Distribution*

The economy of the random model can be improved further if the actual line-strength distribution is approximated with a simple analytic function. This allows the summation over line group in (11) to be replaced by an integral over line strength, so that the equivalent width of all lines in the interval can be found in a single step. The most commonly used analytic line-strength distributions are those introduced by *Goody* [1952, 1964] and *Malkmus* [1967]. Figure 2 shows that the Malkmus distribution provides a better fit to the actual 15-μm band line census, and *Kiehl and Ramanathan* [1983] confirm that random models based on this distribution produce more accurate transmittances than those based on the Goody model. We will therefore consider only models based on the Malkmus distribution. In such models the total equivalent width in a spectral interval is given by

$$w = \int_{-\infty}^{\infty} P(S) w(S, p, T)\, dS \tag{12}$$

where the probability function

$$P(S) = \frac{\Delta\nu}{S\delta} \exp\,[-S/k]$$

and δ and k are constants to be determined from the actual line-strength distribution. In the random models described by *Malkmus* [1967] and *Rodgers* [1968], a Lorentz line shape was assumed:

$$f(\nu) = \frac{\alpha_L}{\pi[\nu^2 + {\alpha_L}^2]} \tag{13}$$

With (12) and (13) the transmission function becomes

$$\tau(p, p') = \exp\left\{-\frac{\pi\alpha_L}{2\delta}\left[\left(1 + \frac{4k\bar{m}}{\pi\alpha_L}\right)^{1/2} - 1\right]\right\} \tag{14}$$

In this equation we have adopted the convention of *Rodgers* [1968] and have defined the quantities

$$\frac{k}{\delta} = \frac{\sum S_i}{\Delta\nu} \tag{15}$$

and

$$\frac{\pi\alpha_L}{\delta} = \frac{4}{\Delta\nu}\frac{[\sum (S_i\alpha_{Li})^{1/2}]^2}{\sum S_i} \tag{16}$$

With these definitions the functional form of the Malkmus random model has strong and weak limits that are identical to those obtained for the *Goody* [1952] random model. The line strengths S_i and the half-widths α_{Li} in (15) and (16) were obtained from the AFGL line-parameter compilation, and their dependence on pressure and temperature along atmospheric optical paths was parameterized by the Curtis-Godson approximation [*Rodgers and Walshaw*, 1966]. (The band parameters k/δ and $\pi\alpha_L/\delta$ used in this investigation are available from the authors.)

Equation (14) provides an efficient method for finding narrow-band transmittances for atmospheric paths with mean pressures greater than about 10^{-2} atm. At lower pressures this standard Lorentz-Malkmus model seriously underestimates the absorption, since it neglects Doppler line-broadening effects. One simple method for improving the low-pressure performance of this model was proposed by *Fels* [1979]. In Fels' model the Lorentz line shape (equation (13)) is replaced by the approximate Voigt line shape given in (6). For that line shape the Malkmus model assumes the form:

$$\tau(p, p') = \exp\left\{\frac{-2}{\pi}\left[\left(\frac{k\bar{m}}{\delta}\right)\left(\frac{\pi\alpha_L}{\delta}\right)\right]^{1/2} \cdot \tan^{-1}\left[\frac{2\delta}{\pi\nu_0}\left(\left(\frac{k\bar{m}}{\delta}\right)\left(\frac{\pi\alpha_L}{\delta}\right)\right)^{1/2}\right] - \frac{\nu_0}{2\delta}\ln\left[\frac{1 + 4(k\bar{m}/\delta)(\delta/\nu_0)\nu_0 C}{1 + 4/\pi^2(k\bar{m}/\delta)(\delta/\nu_0)^2(\pi\alpha_L/\delta)}\right]\right\} \tag{17}$$

The functional form of (17) differs somewhat from that given by *Fels* [1979], since we used the band parameter definitions given by (15) and (16) instead of those used by Fels. This expression is more complicated than the general random model (equations (10) and (11)) but still provides a more efficient band-modeling technique, since it must be evaluated only once in a given 5 cm^{-1} wide spectral interval. In section 3.3 we show that the low-pressure performance of this Fels-Malkmus random model is significantly better than that of the standard Lorentz-Malkmus model for optical paths in atmospheres with small CO_2 mixing ratios. For pure CO_2 atmospheres, (17) still underestimates the absorption at low pressures. We describe a Malkmus model Voigt correction that performs well for all CO_2 mixing ratios in sections 2.6 and 3.3.

2.4. *The Exponential Wideband Model*

Another significant improvement in the efficiency of random models can be achieved if they can be applied to very broad spectral intervals. This can be done only if the wave number dependence of the band parameters k/δ and $\pi\alpha_L/\delta$ can be accounted for in a simple way. One solution to this problem is proposed by *Edwards and Menard* [1964*a*, *b*]. Edwards and Menard show that the line strength decreases almost exponentially with distance away from the center of many infrared absorption bands, while the quantity α_L/δ remains almost con-

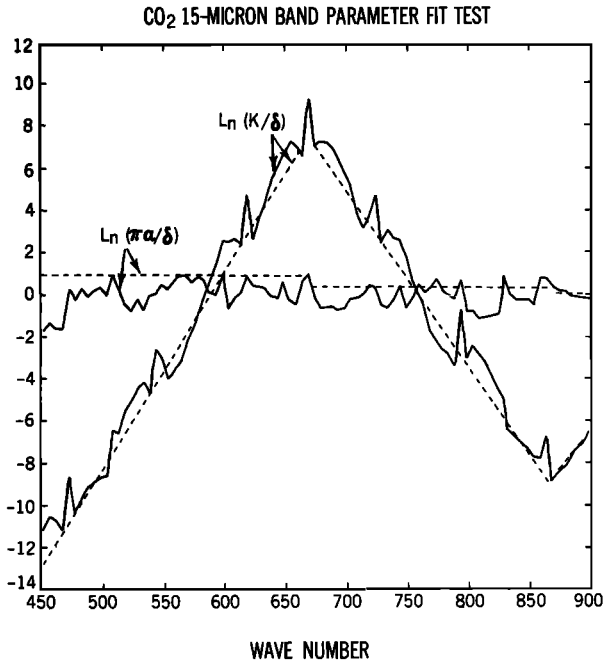

Fig. 3. The CO_2 15-μm band parameters are shown at 5 cm^{-1} resolution for the spectral region extending from 450 to 900 cm^{-1} (solid lines). The parameter k/δ decreases almost exponentially with wave number as one moves away from the band center (667 cm^{-1}). Beyond 870 cm^{-1}, k/δ begins to increase once again because of the 10.4-μm CO_2 hot band. The quantity α_L/δ is shown as an almost horizontal line through the center of this figure. The values of k/δ and α_L/δ adopted for the exponential wideband model (section 2.4) are shown as dashed lines. Values of k/δ are given in square centimeters per gram.

stant throughout the band. For such bands the wave number dependence can be approximated by

$$\frac{k}{\delta}(\nu) \cong S_0 \exp\,[b(\nu - \nu_0)] \tag{18}$$

$$\frac{\pi\alpha_L}{\delta} \cong B = \text{constant} \tag{19}$$

S_0 is the value of k/δ at wave number ν_0, and b is the slope factor defined by

$$b = \frac{d}{d\nu}\left[\ln\left(\frac{k}{\delta}\right)\right] \cong \left\{\ln\left[\frac{k}{\delta}(\nu_1)\right] - \ln\left[\frac{k}{\delta}(\nu_0)\right]\right\}\Big/\Delta\nu \tag{20}$$

where $\Delta\nu = \nu_1 - \nu_0$. The validity of this simple parameterization for the CO_2 15-μm band is illustrated in Figure 3.

Wang [1983] shows that when this simple wave number dependence is incorporated into the Malkmus random model, the transmission function for an entire band can be expressed as a single analytic function. Here we generalize this approach so that it can be used to find the transmittance in any broad segment of an absorption band. When (18) and (19) are inserted into (14) and the resulting expression is integrated from wave number ν_0 to ν_1, we obtain:

$$\tau(p, p') = \frac{1}{\Delta\nu}\int_{\nu_0}^{\nu_1} \exp\left\{-Bp\left[\left[1 + \frac{S_0 m}{Bp} \cdot \exp\,(b(\nu - \nu_0))\right]^{1/2} - 1\right]\right\} d\nu$$

This integral can be evaluated by introducing the change of variables:

$$y = \left\{1 + \frac{S_0 m}{Bp}\exp\,[b(\nu - \nu_0)]\right\}^{1/2}$$

The frequency-integrated transmission function is then

$$\tau(p, p') = \left\{\frac{1}{\Delta\nu}\,[E_1(Bp(y_1 - 1)) - E_1(Bp(y_2 + 1)) + \exp\,(2Bp)[E_1(Bp(y_1 + 1)) - E_1(Bp(y_2 + 1))]]\right\} \tag{21}$$

where

$$y_2 = \left[1 + \frac{S_0 m}{Bp}\exp\,(b\,\Delta\nu)\right]^{1/2}$$

$$y_1 = \left(1 + \frac{S_0 m}{Bp}\right)^{1/2}$$

and E_1 is the first exponential integral [*Abramowitz and Stegun*, 1964].

This simple model can be applied to atmospheric optical paths, where pressure, temperature, and gas mixing ratios may vary, by replacing the absorber amount m with its path-length-integrated value $\bar{m}$ (equation (4)) and replacing the pressure p with its mean value,

$$\bar{p}(p, p') = \frac{1}{\bar{m}}\int_p^{p'} p''\, dm$$

The temperature dependence of the band parameters k/δ and $\pi\alpha/\delta$ is illustrated in Figure 4. From these results we see that the line-width factor B varies little with temperature and can be considered constant, while the magnitude of the slope b (equation (20)), decreases significantly with increasing temperature. We found by trial and error that the temperature de-

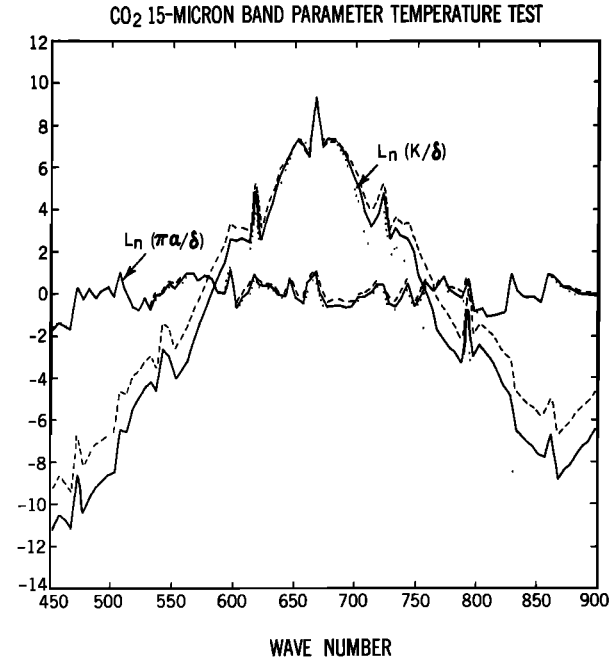

Fig. 4. The quantities k/δ and α_L/δ are shown for temperatures of 200 (dotted line), 250 (solid line), and 300 K (dashed line). In this temperature range the slope of ln (k/δ) decreases almost linearly with temperature, while $\pi\alpha_L/\delta$ has almost no temperature dependence.

TABLE 2. Band Parameters for Exponential Wideband Model Evaluated at 250 K

ν, cm^{-1}	S_0, cm^2 g^{-1}	b	B, atm^{-1}	ε	η, T^{-1}
450–665	2.77227×10^{-6}	19.89672	2.48570	0.8	-4.3×10^{-4}
665–670*	1.23108×10^{4}	...	2.76838	...	...
670–870	1.29753×10^{3}	−16.31618	1.49931	0.83	-3.3×10^{-4}
870–900	2.48811×10^{-4}	6.169583	1.539300	0.7	0.0

*In this interval a standard Lorentz-Malkmus model is used instead of the exponential wideband model. Here $S_0 = k/\delta$, and $B = \pi\alpha_L/\delta$.

pendence of b could be approximated by a function of the form

$$b(T) = \frac{b(T_0)}{\bar{m}} \int_p^{p'} \frac{T}{T_0} f(T)\, dm$$

where

$$f(T) = \varepsilon + \eta T$$

The constants ε and η are listed in Table 2 for the spectral intervals 450–665, 670–870, and 870–900 cm^{-1}. With these values this simple method for approximating the temperature dependence of the CO_2 15-μm band rarely produces absorption errors larger than 10% at temperatures between 120 and 750 K.

This exponential wideband model is more versatile and accurate than those described by *Edwards and Balakrishnan* [1973] and *Wang* [1983], since it can be applied to individual sections of absorption bands as well as to the entire band. This change facilitates the use of different values of $|b|$ on either side of the band center to account for the band asymmetry, and allows the complicated structure of the region occupied by the Q branch of the 15-μm fundamental to be considered separately.

For the tests presented in section 3.4 the exponential wideband model was used to find the broadband transmittance in three spectral intervals extending from 450–665, 670–870, and 870–900 cm^{-1}. A narrow-band Malkmus random model (equation (14)) was used to find the transmission in the spectral interval 665–670 cm^{-1}, which is occupied by the Q branch of the 15-μm fundamental. Values for the broadband model parameters B, $b(T_0)$, and S_0 were obtained by fitting (21) to synthetic spectra generated with the narrow-band Malkmus model. A nonlinear least squares fitting method described by *Bevington* [1969] was used to produce a "best" fit to a data set that included transmittances along paths with absorber amounts and pressures similar to those encountered in atmospheres with CO_2 mass mixing ratios ranging from 0.0005 to 1.0 at pressures between 10^{-6} and 1 atm. This least squares search was initialized with the actual values of k/δ and α_L/δ at the boundaries of the spectral intervals cited above. These quantities were derived from data in the 1978 version of the AFGL line-parameter compilation. The final adopted values of B, b, and S_0 are listed in Table 2, and the band structure obtained with these values is compared to the actual wave number dependent structure of the CO_2 15-μm band in Figure 3.

2.5. *Empirical Logarithmic Wideband Models*

The simplest class of broadband models considered here are the empirical absorption correlation functions. Unlike the band models described above, which approximate the structure of the CO_2 15-μm band, these methods are interpolation formulas that connect the observed linear, square root, and logarithmic regions of the curve of growth of this band. Because of their efficiency and simplicity, such methods have been widely used in studies of atmospheric radiative transfer [*Goody and Belton*, 1967; *Cess and Ramanathan*, 1972; *Ramanathan and Cess*, 1974; *Ramanathan*, 1976; *Ramanathan and Coakley*, 1978; *Kiehl and Ramanathan*, 1983; *Kasting et al.*, 1984]. *Cess and Tiwari* [1972] review these methods and show that they usually assume a simple logarithmic functional form:

$$A(p, p') = A_0 \ln [1 + f(m, p, T)] \tag{22}$$

where

$$A(p, p') = \Delta\nu[1 - \tau(p, p')]$$

is the band-integrated absorption.

A number of functional forms for $f(p, p')$ have been adopted in these models. *Goody and Belton* [1967] use

$$f = [\beta u/(u + 4\beta)]^{1/2}$$

where

$$u = \sum S_i m / A_0$$

and

$$\beta = 4\alpha_L/\delta$$

are a dimensionless path length and the ratio between the mean line width and line spacing, respectively.

Cess and Tiwari [1972] note that this function approaches the wrong asymptotic limit for $\beta \gg 1$, and they suggest the alternate form:

$$f = u[2 + (u + u/\beta)]^{-1/2}$$

This formulation is used in studies of the Martian and Venusian atmospheres by *Cess and Ramanathan* [1972].

A modified form of this expression is employed by *Kiehl and Ramanathan* [1983]. Their model explicitly accounts for four CO_2 isotopes and 13 hot bands in addition to the CO_2 15-μm fundamental, and it includes a parameterization for partial overlap between these different bands. For a given isotope i and band j the function $f_{i,j}$ has the form

$$f = u_{i,j}[4 + u_{i,j}(1 + 1/\beta_{i,j})]^{-1/2} \tag{23}$$

The complete expression for the broadband absorption is given by

$$\begin{aligned} A = 2A_0 \Bigg\{ & \ln\left[1 + \sum_{i=1}^{4} (f_{i1} + f_{i4} + f_{i5} + f_{i9} + f_{i11} + f_{i12})\right] \\ & + T_1 \Bigg[\ln\left(1 + \sum_{i=1}^{4} (f_{i2} + f_{i14})\right) \\ & + \ln\left(1 + \sum_{i=1}^{4} (f_{i3} + f_{i13})\right)\Bigg] \\ & + T_2 \left[\ln\left(1 + \sum_{i=1}^{4} f_{i7}\right) + \ln\left(1 + \sum_{i=1}^{4} f_{i8}\right)\right] \\ & + T_3 \left[\ln\left(1 + \sum_{i=1}^{4} f_{i10}\right) + \ln\left(1 + \sum_{i=1}^{4} f_{i6}\right)\right]\Bigg\} \end{aligned}$$

where T_1, T_2, and T_3 account for the effects of partially overlapped bands. These quantities are derived in an appendix to *Kiehl and Ramanathan* [1983]. This equation was repeated here only because the braces shown above were neglected in that paper (J. Kiehl, personal communication, 1984). For the tests presented in section 3.5 we adopted the band parameters

listed by *Kiehl and Ramanathan* [1983, Table 1]. Of these parameters the total line strength $\sum S_i$, the mean half-width α_L, and the mean line spacing δ were obtained from the AFGL line-parameter compilation for the spectral interval extending from 500 to 800 cm^{-1}. The constant A_0 was derived by fitting this model to laboratory measurements of total band absorptance [*Edwards*, 1960].

In spite of its apparent complexity this expression provides an efficient method for finding the CO_2 15-μm band absorptance, since it must be evaluated only once for the entire band. In section 3.5 we show that this model produces accurate results for optical paths at pressures between 0.01 and 1 atm, but it performs poorly for low-pressure paths because Voigt line-shape effects have been neglected. One simple method for including these effects is described by *Ramanathan* [1976]. We describe an alternate approach in section 2.6.

Another, simpler logarithmic model for the CO_2 15-μm band is used by *Pollack et al.* [1981] in studies of the Martian general circulation. This model has the form:

$$A(p, p') = d\left(\frac{T}{T_0}\right)^{q_d} \ln\left[1 + g\left(\frac{T}{T_0}\right)^{q_f} m^b p^a\right] \tag{24}$$

where $d = 64.4$, $q_d = 0.879$, $q_f = -0.256$, $g = 0.153$, $b = 0.566$, and $a = 0.323$ are constants obtained by fitting (24) to laboratory measurements of 15-μm band absorption [*Howard et al.*, 1955; *Burch et al.*, 1962]. Here m is the absorber path length (cm atm), T is temperature (Kelvin), and p is the pressure (in mbar). In section 3.5 we show that this simple empirical model performs poorly for atmospheric optical paths with pressures and absorber amounts outside the range of values included in the fitted data sets.

2.6. *Doppler and Voigt Effects in Narrow-Band and Broadband Models*

A simple method for improving the low-pressure performance of both narrow-band and broadband models can be derived from the Voigt parameterization described by *Rodgers and Williams* [1974]. Rodgers and Williams show that the equivalent width of a single Voigt line can be approximated by the interpolation formula:

$$w_V = [w_L^2 + w_D^2 - (w_L w_D/\textstyle\sum Sm)^2]^{1/2} \tag{25}$$

where w_L and w_D are Lorentz and Doppler equivalent widths of the line, respectively, and $\sum Sm$ is its "weak-line" equivalent width. Rodgers and Williams show that this simple interpolation formula rarely produces equivalent width errors larger than 8%.

Here we modified (25) to give the Voigt absorption in a broad spectral region containing many lines, so that it could be used with band models like those described above. In our method, separate band models were first used to find the Lorentz, Doppler, and weak-line absorption in a given spectral interval. The Voigt absorption was then obtained from the relation

$$A_V = [A_L^2 + A_D^2 - (A_L A_D/A_W)^2]^{1/2} \tag{26}$$

where

$$A_x = \Delta\nu(1 - \tau_x)$$

and τ_x is the transmittance for the spectral interval.

The weak-line absorption in a spectral interval was given by

$$A_W = \Delta\nu[1 - \exp(-\textstyle\sum S_i m/\Delta\nu)] \tag{27}$$

The Lorentz absorption in narrow spectral intervals was found with the standard Lorentz-Malkmus random model (equation (14)). The exponential wideband model (equation (21)) provides an accurate method for finding the Lorentz absorption in wider spectral intervals.

Approximate methods for finding the Doppler absorption were developed from the following considerations. At low pressures where Doppler effects are important, absorption lines are sufficiently narrow that line overlap is not important except in the narrow spectral intervals occupied by Q branches. This facilitates the development of Doppler band models, since a parameterization of overlap is not needed. Unfortunately, this lack of line overlap also complicates the development of these models, since even the very weak lines, which are no longer buried in the wings of nearby strong lines, can contribute significantly to the total Doppler absorption. Doppler band models will therefore be much more sensitive to the choice of line-strength distribution than Lorentz band models. Errors resulting from the use of the Malkmus line-strength distribution, instead of the actual distribution for the CO_2 15-μm band, are demonstrated in section 3.3.

These considerations suggest that a general random model (section 2.2) must be used if accurate Doppler transmittances are needed. The efficiency of such models can be improved significantly for low-pressure applications, since the frequency dependence of the line strength (i.e., the band contour) can be ignored without introducing large errors in the treatment of line overlap. A Doppler general random model can therefore be used to find transmission in spectral intervals much wider than 5 cm^{-1} in a single step. In the nonoverlapping limit it is frequency variations in the temperature dependence of the line strength (Figure 4) instead of the shape of the band contour that limits the width of the spectral interval that can be used in the general random model. If the temperature varies along a low-pressure optical path and the *Rodgers and Walshaw* [1966] temperature correction method is used, this model can produce accurate (<5% errors) transmittances in spectral intervals as wide as 50 cm^{-1}. If the temperature along the path is constant and the band parameters are derived for this temperature, the Doppler general random model can be used to give the transmission within the entire 15-μm band (450–900 cm^{-1}) in a single step.

The efficiency of the Doppler general random model can be improved further if a simple parameterization for the equivalent width of a Doppler line is used. Here we used the Doppler limit ($\alpha_L \to 0$) of the *Fels* [1979] approximate Voigt line shape (equations (5) and (6)). In this limit the equivalent width of a Doppler line is given by

$$w_D \cong 2\beta\alpha_D\{1 - \exp[-Sm/(2\beta\alpha_D)]\} \tag{28}$$

When this expression is incorporated into (11) the following general random model for Doppler lines is obtained:

$$\tau_D = \left\{\exp\left[-2\beta \sum_{j=1}^{J} n_j\alpha_{Dj}[1 - \exp(-Sm/(2\beta\alpha_{Dj}))]\right]\right\} \tag{29}$$

To find the Voigt absorptance for the CO_2 15-μm band, we first used this expression to find the Doppler absorption in nine 50 cm^{-1} wide spectral intervals between 450 and 900 cm^{-1}. These results were summed to give the total Doppler absorption. The narrow-band Lorentz-Malkmus model (equation (14)) was then used to find the Lorentz absorption in ninety 5 cm^{-1} wide spectral intervals between 450 and 900 cm^{-1}. These results were then summed to give the total Lorentz absorption A_L. Finally, (26) and (27) were used to combine the broadband Doppler and Lorentz results to give the

approximate Voigt absorption in this band. The performance of this hybrid Voigt random model is demonstrated in section 3.3. There we show that this model produces more accurate low-pressure results than the Fels-Malkmus random model, since it uses a more realistic line-strength distribution in the Doppler regime.

This method is relatively versatile, since it allows one to find the Voigt absorption within an entire band or any small fraction of it. This model can also be used to find transmittances for infrared-absorbing gases other than CO_2 (H_2O, SO_2, O_3, etc.). If only the broadband Voigt absorption within the CO_2 15-μm band is needed, the efficiency of this hybrid method can be improved as follows. First, the narrow-band Malkmus model that is used to find the Lorentz absorption can be replaced with the exponential wideband model (equation (21)) or some other more efficient broadband model for Lorentz lines. Second, the actual line-strength distribution used in the Doppler general random model can be replaced with an approximate analytic function that accurately models the census of lines in this band. We have derived one such function as a generalization of the Goody and Malkmus distributions.

In the Goody and Malkmus line-strength distributions the number of lines with strengths between S and $S \pm dS$ is given by

$$SP(S) \propto S^{\gamma} \exp(-S/k)$$

where γ is a constant which can assume values of 0 (Malkmus) or 1 (Goody). These functions are compared to the actual line-strength distribution for the entire CO_2 15-μm band in Figure 2. There we see that the Malkmus distribution provides a somewhat more accurate fit but that both approximate distributions severely underestimate the number of weak lines in this band. A much better approximation to the 15-μm line census can be obtained by combining a Goody distribution for strong lines ($S \geq 100$ cm^2 atm gm^{-1}) and a distribution with $\gamma = -1/4$ for weaker lines,

$$SP(S) = S\,\Delta\nu\,(k\delta)^{-1} \exp(-S/k) + S^{-1/4}\psi \exp(-S/l) \qquad (30)$$

This function is also shown in Figure 2. It was not possible to derive a simple band model based on this line-strength distribution and a general approximate Voigt line shape, but the following technique provides a simple method for finding transmittances in the Doppler regime.

In the Doppler limit the *Fels* [1979] approximate Voigt line shape (equation (6)) becomes a simple rectangular line with half-width equal to $v_0 = \beta\alpha_D$ and height equal to $C = (2\beta\alpha_D)^{-1}$. For this line shape the random model transmission function for a band with the above line-strength distribution is

$$\tau_D(p, p') = \left\{\exp\left[-\frac{km}{\delta}\left(1 + \left(\frac{km}{\delta}\right)\left(\frac{\delta}{2\beta\alpha_D}\right)\right)^{-1} + 2\beta\alpha_D\Gamma(-1/4)l^{-1/4}\psi\left(\left(1 + \frac{lm}{2\beta\alpha_D}\right)^{1/4} - 1\right)\right]\right\} \qquad (31)$$

Here $\Gamma(-1/4) = 4.90167$ is the gamma function, and the quantities k, δ, ψ, and l were found by fitting (30) to the line census shown in Figure 2. This line census includes all CO_2 lines in the spectral region extending from 450 to 900 cm^{-1}. We found that $k = 756$ cm^{-1} cm^2 g^{-1}, $\delta = 4.2$ cm^{-1}, $\psi = 0.6333$, and $l = 64.039$ cm^{-1} cm^2 g^{-1} produced an acceptable fit at 250 K.

The first term in the exponential in (31) is simply the Doppler limit of a random model that employs the Goody line-intensity distribution and the *Fels* [1979] approximate Voigt line shape. The second term in the exponential is an additional contribution that accounts for absorption by the large number of weak lines in this band.

The Curtis-Godson approximation [*Rodgers and Walshaw*, 1966] was used to parameterize the temperature dependence of the mean line strengths k and l. We found that it was necessary to employ different temperature corrections for the Goody and $S^{-1/4}$ components of this model, since the temperature dependence of the lines in these two distributions is significantly different. Most of the strong lines in the Goody distribution are members of the temperature insensitive CO_2 15-μm fundamental band, while most of the weaker lines in the $S^{-1/4}$ distribution are members of hot bands.

The simple Doppler model given in (31) provides an economical method for improving the low-pressure performance of the broadband models described in sections 2.4 and 2.5. In section 3.4 we test the accuracy of a hybrid broadband model that uses the modified *Rodgers and Williams* [1974] Voigt interpolation formula (equation (26)) to combine the Doppler results from (31) with Lorentz results from an exponential wideband model (section 2.4). We find that this new broadband model provides a reliable method for finding CO_2 15-μm band transmittances over a broad range of pressures, temperatures, and path lengths.

2.7. *The Model Atmosphere*

Our model atmospheres have 109 vertical levels at pressures between 10^{-6} and 1.0 atm. At pressures less than 10^{-1} atm, levels are evenly spaced in ln (p) and there are 15 levels per decade of pressure. At pressures greater than 10^{-1} atm, levels are also evenly spaced in ln (p), but there are 30 levels per decade of pressure. Two model atmospheres with constant CO_2 mass mixing ratios of 0.0005 and 1.0 were used in the comparisons presented in section 3. Line-by-line model results were not available for model atmospheres with other CO_2 mixing ratios, but we compared results from the general random model to those from the simpler approximate methods for a variety of mixing ratios, including $r = 0.001$, 0.002, 0.005, and 0.05 (i.e., the 2X, 4X, 10X, and 100X terrestrial CO_2 cases). Errors produced in these tests generally fell within the range of those obtained for the extreme cases described in next section 3.

The U.S. Standard Atmosphere (1976) temperature profile was used for all tests presented here. This profile was chosen because its structure and range of values (180–295 K) provided a rigorous test of parameterizations for temperature dependence used in the approximate methods. Experiments employing isothermal model atmospheres at 200, 250, and 300 K were also used to help interpret these temperature effects.

3. RESULTS AND DISCUSSION

To determine the accuracy and range of validity of the approximate methods described in sections 2.2–2.6, we proceeded as follows. First, each method was used to find the 15-μm band transmittance between each level and all other levels in model atmospheres with mixing ratios of $r = 0.0005$ and $r = 1.0$. These transmittances were obtained along paths at four different zenith angles, and Gaussian quadrature was used to integrate these results over zenith angle to give transmittances in flux form. These results were then converted from transmittances to broadband (450–900 cm^{-1}) absorptances, defined by

$$A_i(p, p') = \Delta\nu[1 - \tau(p, p')]$$

and compared with the corresponding results obtained from the "exact" line-by-line model. The difference between exact

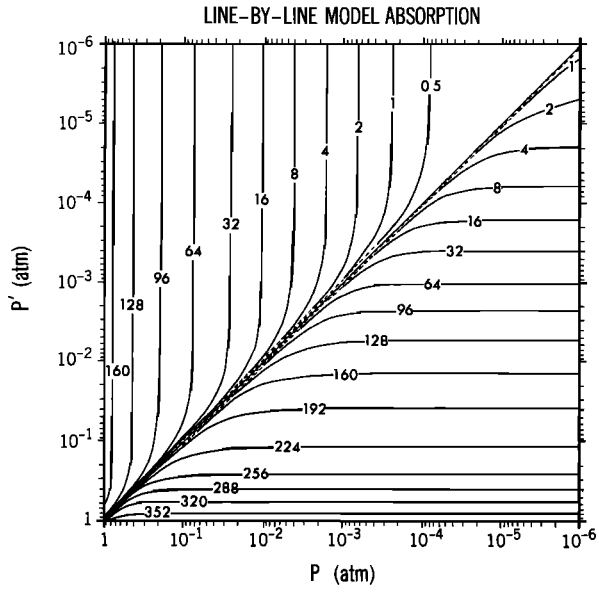

Fig. 5. The band absorptance in the wave number interval 450–900 cm^{-1}, computed with the Fels-Schwarzkopf line-by-line model. The absorptance between each model level p and all other levels p' is shown for atmospheres with CO_2 mass mixing ratios of 0.0005 and 1.0. Values obtained for the present terrestrial CO_2 amounts ($r = 0.0005$) are plotted in the upper left-hand corner of the diagram above the $p = p'$ line. Results obtained for the pure CO_2 atmosphere are plotted below this line.

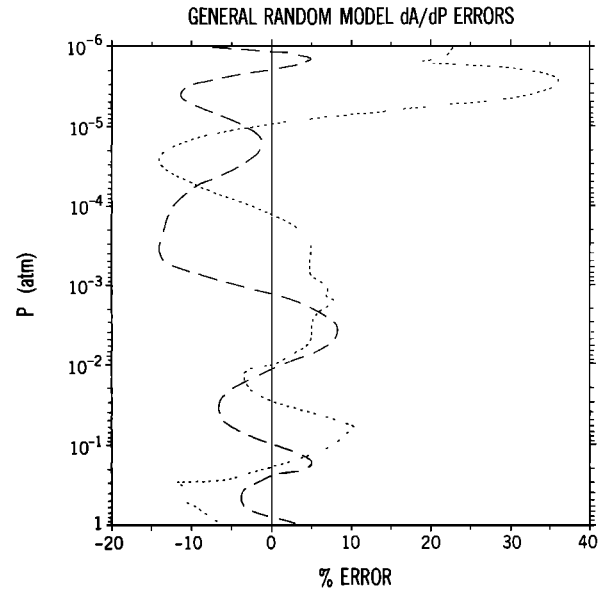

Fig. 7. Errors in the vertical derivative of the general random model absorptance, $Q_t = dA(p, 0)/dp$, defined by $E_Q = 100\ (Q_t - Q_{LBL})/Q_{LBL}$ are shown as a function pressure. Results for model atmospheres with CO_2 mass mixing ratios of 0.0005 (dashed line) and 1.0 (dotted line) are shown. This convention is used in all subsequent plots of Q (Figures 9, 11, 13, 15, 17, and 19).

(A_{LBL}) and approximate absorption (A_t) was then expressed as a percentage error, defined by

$$\text{Err}\ (p, p') = 100\ (A_t - A_{LBL})/A_{LBL}$$

These errors are displayed in contour plots (Figures 6, 8, 10, 12, 14, 15, and 18) of error versus p and p'. Because these plots are symmetric about the line $p = p'$, we chose to conserve space and present the results for both the terrestrial and pure CO_2 mixing ratio cases on the same figure. For all of the contour plots, errors for the terrestrial model atmosphere ($r = 0.0005$) occupy the upper left-hand region above the $p = p'$ line. Absorption errors along paths in the pure CO_2 model atmosphere are displayed in the lower right-hand region, below the $p = p'$ line.

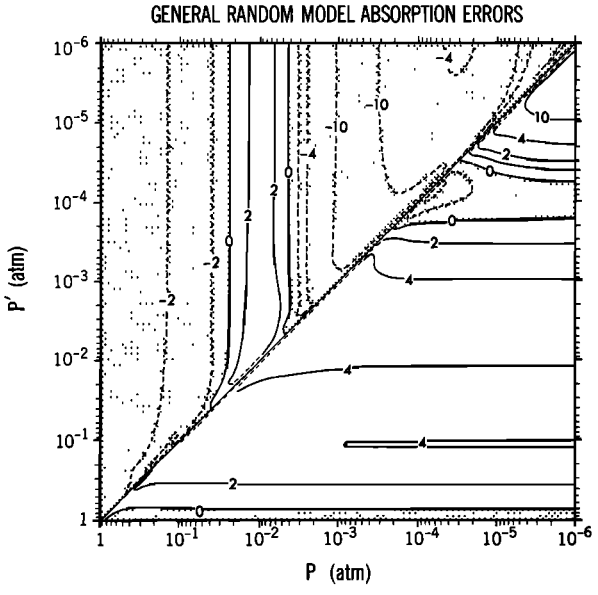

Fig. 6. Differences between the band absorptance computed with the general random model and that obtained from the line-by-line model are shown. These differences are expressed as percentage errors, defined by $E_A = 100\ (A_t - A_{LBL})/A_{LBL}$. Absorptance errors along paths between each layer p and all other layers p' are shown for model atmospheres with CO_2 mass mixing ratios of $r = 0.0005$ and $r = 1.0$. As in Figure 5, the results for $r = 0.0005$ are plotted above the $p = p'$ diagonal. Errors along paths in the pure CO_2 atmosphere are shown below this line. Regions where A_t is less than A_{LBL} are shaded. All subsequent contour plots of absorption errors (Figures 8, 10, 12, 14, 16, and 18) use this format.

Because many of the approximate methods described above have been used to find atmospheric cooling rates, we also tested their accuracy for this application. In general, radiative cooling rate errors will depend on the atmospheric temperature structure as well as the accuracy of the band model used. This dependence on temperature will not be significant, however, if the atmosphere is optically thin ($A \rightarrow 0$) or if the temperature varies slowly with pressure. In these cases, cooling to space will dominate, and cooling rate errors will be proportional to the quantity $Q = dA(p, 0)/dp$. We used each of the models described above to compute this quantity. These results were then compared to those obtained from the line-by-line model and differences were expressed as percentage errors in Figures 7, 9, 11, 13, 15, 17, and 19. Here errors in dA/dp for a terrestrial CO_2 mixing ratio are plotted as a dashed line. A dotted line is used to show dA/dp errors for a pure CO_2 model atmosphere.

3.1. *The Line-by-Line Model*

In Figure 5 we show the frequency-integrated (450–900 cm^{-1}) 15-μm band absorption computed with the Fels-Schwarzkopf line-by-line model. These results are used as the standard ("exact") values in all subsequent comparisons. The upper left-hand half of Figure 5 shows the absorption between each pressure level p and any other level p' for an atmosphere with the present terrestrial CO_2 mixing ratio ($r = 0.0005$). The lower right-hand half of the plot shows the absorptance in a pure CO_2 atmosphere ($r = 1.0$). For the terrestrial CO_2 mixing ratio we obtain a maximum absorptance of 180 cm^{-1}

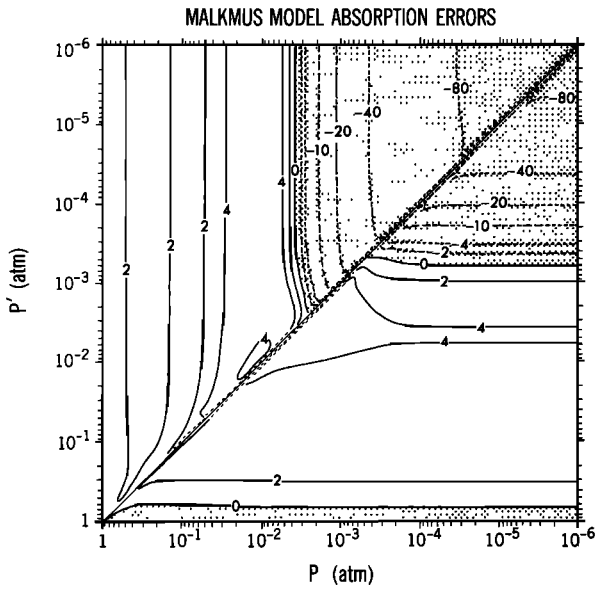

Fig. 8. Absorptance errors for a narrow-band random model that incorporates the Malkmus line-strength distribution and a Lorentz line shape. As in Figure 6, errors in a model atmosphere with a CO_2 mass mixing ratio of 0.0005 are plotted above the $p = p'$ diagonal. Absorptance errors for the pure CO_2 model atmosphere are plotted below this line.

along paths between lowest level (1 atm) and the top of the atmosphere. More than 98% of this absorption occurs in the spectral region between 550 adn 850 cm^{-1}. For other paths in this atmosphere, an even larger fraction of the absorption is confined to this spectral region. This observation suggests that CO_2 15-μm band absorption outside of this spectral interval can be neglected in some studies of terrestrial radiative transfer.

The lower right-hand half of Figure 5 shows that this is not true for atmospheres with large CO_2 mixing ratios. There we see that the absorption along paths between the 1-atm level and space approaches 400 cm^{-1}. In such atmospheres much of the thermal cooling at pressures greater than 0.1 atm results from transfer within the far wings of this band. An accurate treatment of the entire CO_2 15-μm band (along with the 9.4- and 10.4-μm hot bands) is therefore needed in studies of the thermal infrared optical properties and cooling rates of atmospheres with large CO_2 mixing ratios.

3.2. *The General Random Model for Simplified Voigt Lines*

The accuracy of the general random model is demonstrated in Figures 6 and 7. Figure 6 shows that the band-integrated absorption obtained from this model rarely differs from the corresponding line-by-line results by more than 5% for paths with mean pressures greater than 10^{-3} atm, where the effects of line overlap are most pronounced. Errors in the quantity dA/dp (Figure 7) also remain small (<10%) for these paths. These results are significant, since they demonstrate the accuracy of the parameterization for line overlap employed by random models. Recall that these models account for overlap effects by assuming that absorption lines are distributed randomly with wave number throughout each 5 cm^{-1} spectral interval within the CO_2 15-μm band. This approximation is least valid and produces its largest errors in those 5 cm^{-1} wide spectral regions occupied by the Q branches of this band. In these narrow intervals the distributions of line strengths, widths, and spacings vary significantly with wave number. This variation requires that intervals much smaller than 5 cm^{-1} be used if Q branch line overlap is to be properly accounted for by random models. The general random model errors for the terrestrial ($r = 0.0005$) CO_2 mixing ratios are somewhat greater than those for the pure CO_2 case, since the Q branches contribute a larger fraction of the total absorption for small mixing ratios.

Another source of error in random models is the assumption that spectral lines contribute to absorption only in the spectral interval where their centers are located. If line parameters are changing rapidly with wave number, such models cannot accurately account for contributions to the absorption in a given spectral interval by lines outside of that interval. The effect of this assumption is to produce an overestimate of the absorption in spectral intervals occupied by Q branches and an underestimate of absorption in adjacent spectral intervals. Very little of the error in Figures 6 and 7 can be attributed to this factor, however, because CO_2 lines have strongly sub-Lorentzian wings [*Fels and Schwarzkopf*, 1980], and the line-by-line model accounts for this sub-Lorentzian behavior by ignoring contributions from the wings of lines with centers more than 3 cm^{-1} away from the wave number of interest. For gases with super-Lorentzian line profiles, such as H_2O, a more accurate treatment of the far wings of distant lines may be needed if narrow spectral intervals are used. One approach for incorporating these effects in random models is described by *Aoki* [1978].

For optical paths with mean pressures less than 10^{-3} atm the general random model absorptance errors are as large as 10%, and errors in dA/dp sometimes exceed 30%. These errors are caused primarily by deficiencies in the simple parameterization for the Voigt line shape (equation (6)) used in this model. This approximation overestimates the absorption along paths at pressures near 10^{-6} atm and underestimates the absorption along paths at pressures between 10^{-4} and 10^{-3} atm. Unfortunately, we were not able to find or derive a simple random model that incorporates a more accurate description of the Voigt line shape. A model of this kind would be very useful for studies of the upper atmospheres of Vensus, earth, and Mars.

In addition to an approximate treatment of line overlap and line shape, the general random model uses the Curtis-Godson approximation [*Rodgers and Walshaw*, 1966] to account for changes in the line width and strength which are caused by variations in pressure and temperature along atmospheric optical paths. This approximation also adds to the errors seen in Figures 7 and 8, but its contribution was much smaller than those described above. This result is consistent with the conclusions reached by Rodgers and Walshaw.

3.3. *Random Models That Use the Malkmus Line-Strength Distribution*

Comparisons between line-by-line model results and those obtained from narrow-band random models that use the Malkmus line-strength distribution are presented in Figures 8 through 13. The simplest of these models employs the Malkmus line-strength distribution and a Lorentz line shape (equations (13) and (14)). Figures 8 and 9 show that this model usually overestimates the absorption and dA/dp at pressures greater than 10^{-3} atm, but these errors are not much larger than those produced by the much more computationally expensive general random model (Figure 8). One can therefore approximate the actual 15-μm band line-strength distributions with the Malkmus distribution without significantly degrading random model performance for high-pressure optical paths.

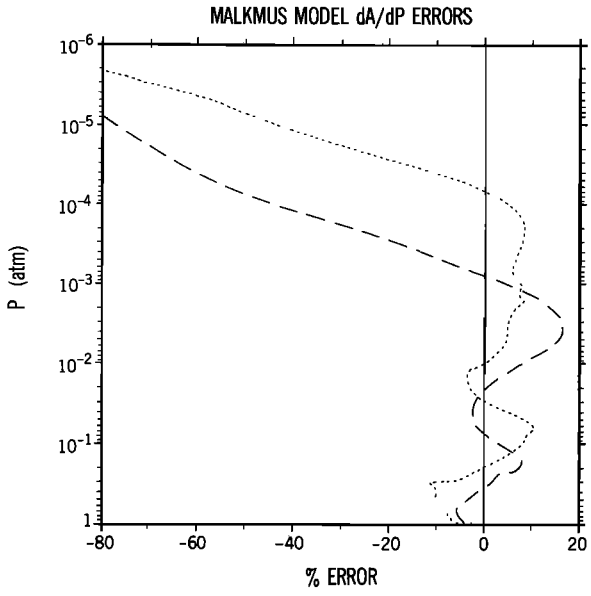

Fig. 9. Errors in the quantity $Q = dA(p, 0)/dp$ for the Malkmus random model described in Figure 8 are shown for model atmospheres with CO_2 mass mixing ratios of 0.0005 (dashed line) and 1.0 (dotted line).

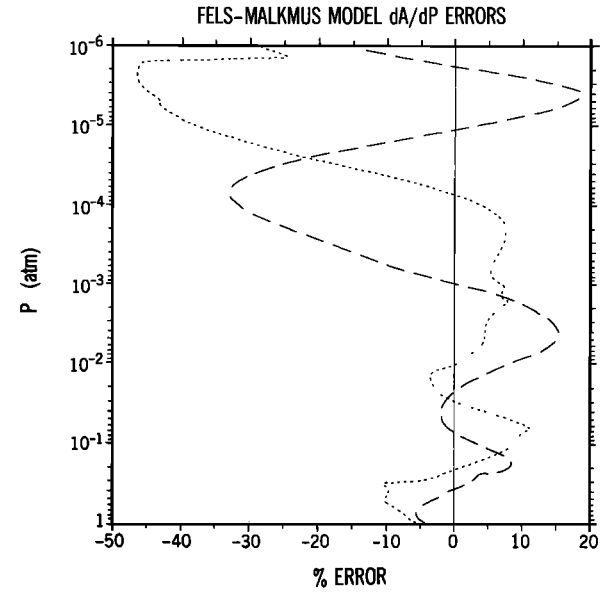

Fig. 11. Errors in the quantity $Q = dA(p, 0)/dp$ for the Fels-Malkmus random model described in Figure 10. The dashed line shows errors for the $r = 0.0005$ case. Errors in the pure CO_2 atmosphere are shown as a dotted line.

For low-pressure optical paths (p, $p' < 10^{-3}$ atm) this simple Lorentz-Malkmus model severely underestimates the absorptance and its vertical derivative. The large errors are produced because this model completely ignores Doppler line-broadening effects. Two simple methods for including a more accurate Voigt line shape in Malkmus random models are tested below.

Results obtained from a Malkmus model that uses the *Fels* [1979] simplified Voigt line shape are shown in Figures 10 and 11. The low-pressure performance of this model is significantly better than that of the Lorentz-Malkmus model, but it is still much worse than that of the general random model. This result was initially surprising, since the Fels-Malkmus and general random models share many similar features, including identical assumptions about line overlap, line shape, temperature dependence, and pressure scaling. The only difference between these models is the line-strength distribution used. Recall that the general random model used a distribution very similar to that observed, while the Malkmus model employed an analytic distribution (equation (12)) with band constants (equations (15) and (16)) chosen to produce accurate results when all lines in a given spectral interval are in the strong- or weak-line limits. The line-strength popu-

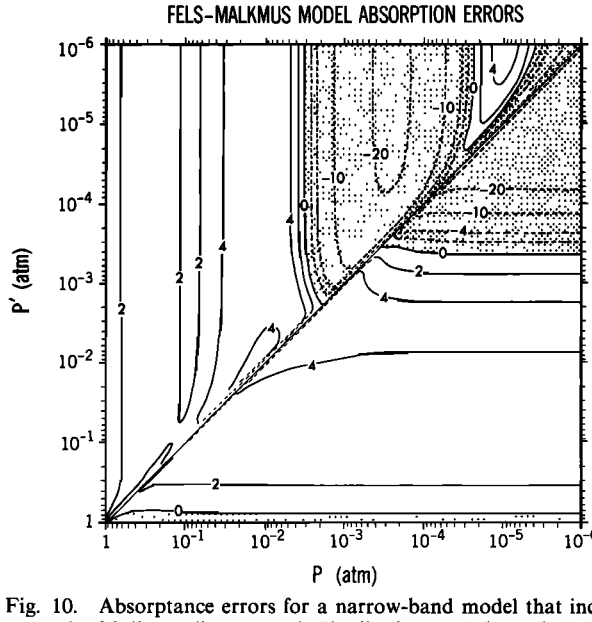

Fig. 10. Absorptance errors for a narrow-band model that incorporates the Malkmus line-strength distribution and the *Fels* [1979] approximate Voigt line shape are shown for model atmospheres with CO_2 mass mixing ratios of 0.0005 (above $p = p'$ diagonal) and 1.0 (below $p = p'$ diagonal).

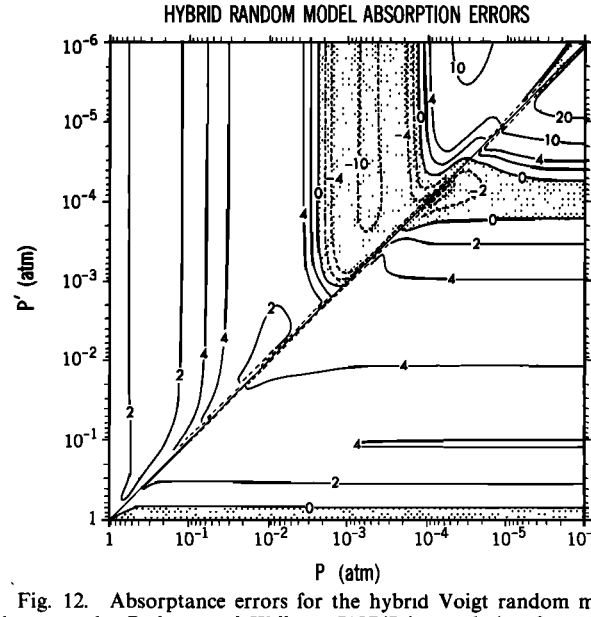

Fig. 12. Absorptance errors for the hybrid Voigt random model that uses the *Rodgers and Williams* [1974] interpolation formula to combine results from a narrow-band Lorentz-Malkmus model with those from a broadband general random model for a simplified Doppler line shape. Errors for the $r = 0.0005$ case are plotted above the $p = p'$ diagonal. Errors for the pure CO_2 atmosphere are plotted below this line.

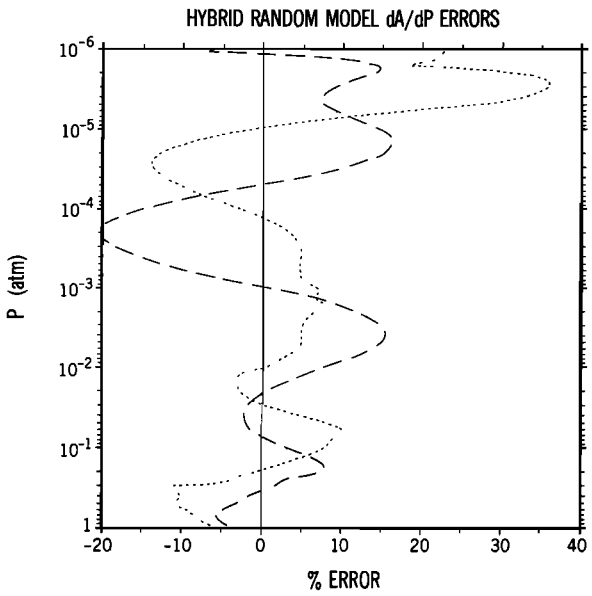

Fig. 13. Same as Figure 11 except for the hybrid Voigt random model described in Figure 12.

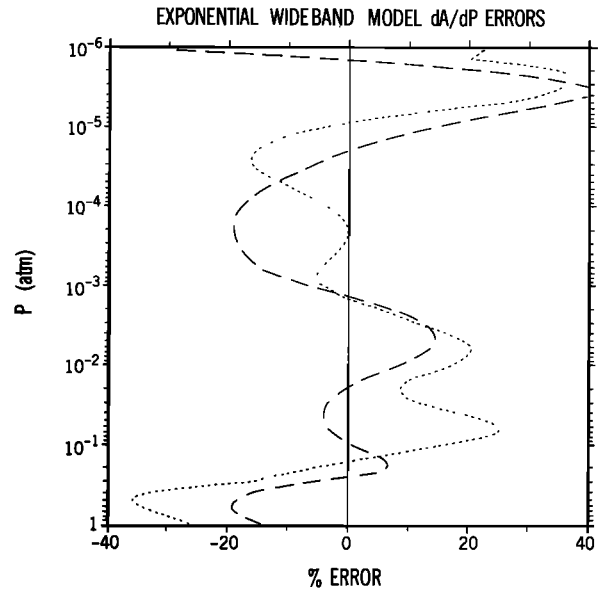

Fig. 15. Same as Figure 11 except for the hybrid wideband model described in Figure 14.

lations can vary significantly from one spectral interval to another in the 15-μm band, but Figure 2 demonstrates the kinds of differences that can occur between the actual distribution and the Malkmus distribution when they are compared for the entire band (450–900 cm^{-1}). For this spectral region the Malkmus distribution slightly overestimates the number of strong lines and seriously underestimates the number of weak lines. This deficiency causes little error at high pressures, since the weaker lines are buried in the pressure-broadened wings of nearby strong lines, so that their effects are less pronounced. At lower pressures, where all lines are narrower, this is no longer the case, and even the weakest lines can contribute

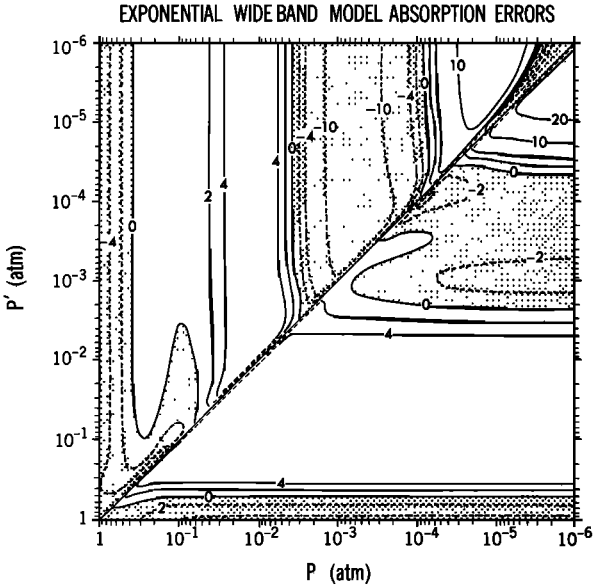

Fig. 14. Absorptance errors for the hybrid wideband random model described in sections 2.4 and 2.6. This model uses a three-interval exponential wideband model (450–665 cm^{-1}, 670–870 cm^{-1}, and 870–900 cm^{-1}) to find the absorptance at high pressures. A simplified wideband Doppler model is used at low pressures. The *Rodgers and Williams* [1974] interpolation formula is used to combine these Lorentz and Doppler results. Errors in the model atmosphere with $r = 0.0005$ are shown above the $p = p'$ diagonal. Errors for the $r = 1.0$ case are shown below this line.

significantly to the total band absorption. This problem would have little effect on the accuracy of the Fels-Malkmus random model if all lines were in the weak limit at these low pressures, but this is not the case in atmospheres with large CO_2 mixing ratios.

A second method for including Doppler and Voigt effects in random models is outlined at the beginning of section 2.6 (equations (14), (26), (27), and (29)). This technique employs the *Rodgers and Williams* [1974] interpolation formula to combine the output from a broadband general random model for Doppler lines with that from the narrow-band, Lorentz-Malkmus model. The accuracy of this method is demonstrated in Figures 12 and 13. Figures 12 and 13 show that this model produces much smaller errors at low pressures than the Fels-Malkmus random model described above. This improved performance is a direct consequence of the fact that the broadband general random model for Doppler lines includes a more accurate description of the CO_2 15-μm line-strength distribution than that used in the Malkmus model.

3.4. *The Exponential Wideband Model*

The broadband model results presented in this section were obtained from a model that incorporates the exponential wideband model for Lorentz lines (section 2.4) and the Voigt parameterization described in (26), (27), and (31). Comparisons between the results obtained from this model and those obtained with the line-by-line model are presented in Figures 14 and 15. Figures 14 and 15 show that this efficient band model can provide a relatively accurate description of CO_2 15-μm absorption over a very broad range of pressures, temperatures, and absorber path lengths.

For paths at pressures greater than 10^{-3} atm much of the error in Figures 15 and 16 is a consequence of the simple temperature dependence employed in the exponential wideband model. These errors are reduced from $< 10\%$ to $\leq 3.5\%$ when results from this model are compared to those from the line-by-line model for an isothermal atmosphere at 250 K. This smaller error reflects the accuracy to which the wave number dependence of the 15-μm CO_2 band can be represented by a simple exponential function.

At pressures less than 10^{-3} atm, where Doppler and Voigt

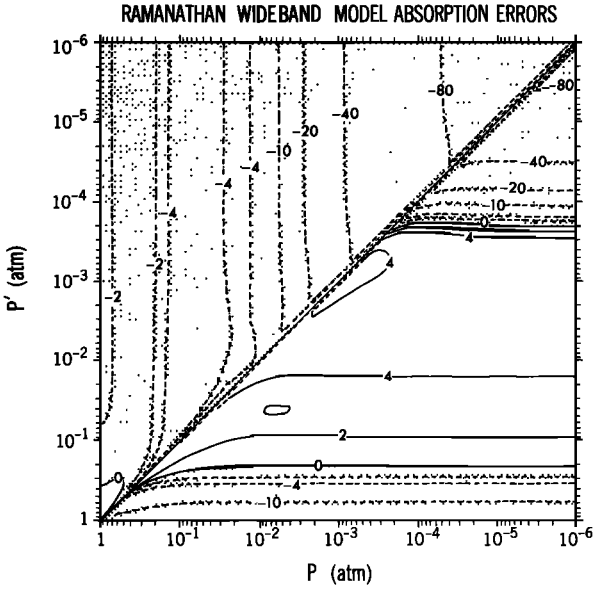

Fig. 16. Absorptance errors for the empirical wideband model described by Kiehl and Ramanathan are shown for the $r = 0.0005$ (above the $p = p'$ diagonal) and $r = 1.0$ (below the $p = p'$ diagonal) cases. This model underestimates the integrated band absorptance at most levels for both low and high CO_2 amounts. The largest errors occur at low pressures, since this model lacks a correction for Doppler line broadening.

effects become important, the broadband model results are very similar to those obtained from the much more expensive narrow-band general random model. Like that model, this broadband model overestimates the absorption by up to 10% for paths at pressures near 10^{-4} atm and underestimates the absorption along paths at pressures below 10^{-5} atm. This model outperforms the Fels-Malkmus random model at these low pressures, since it includes a more accurate description of the CO_2 line-strength distribution.

3.5. *Empirical Logarithmic Wideband Models*

Differences between 15-μm band absorptances obtained from the *Kiehl and Ramanathan* [1983] logarithmic wideband model (equation (23)) and those obtained from the line-by-line model are shown in Figures 16 and 17. There we see that this broadband model underestimates the total absorption at most levels. Much of the error in the absorption A and its derivative dA/dp at pressures less than 10^{-3} atm is produced because this model does not include Doppler line-broadening effects. Its range of validity could therefore be extended significantly if it were combined with the broadband Doppler model described in section 2.6.

At pressures greater than 10^{-3} atm this model never produces absorption errors larger than 10% for the $r = 0.0005$ case, but errors larger than 15% occur for some paths in the pure CO_2 model atmosphere. About half of this high-pressure absorption error can be accounted for by differences in the bandwidth used in this log model and that used for the line-by-line model. Kiehl and Ramanathan assumed that the CO_2 15-μm band was confined to the spectral interval extending from 500 to 800 cm^{-1}, and they derived band parameters only for this interval. In the line-by-line model we included all CO_2 lines in the spectral interval extending from 450 to 900 cm^{-1}. As we noted in section 3.1, there is significant absorption throughout this region for high-pressure paths in pure CO_2 atmospheres. The remainder of the error in the Kiehl and Ramanathan log model is small and is more difficult to account for. We assume that it results from deficiencies in their parameterization for partially overlapped bands or from small errors in the specification of the empirical band constant A_0.

Results obtained with the *Pollack et al.* [1981] logarithmic broadband model (equation (24)) are compared to those from the line-by-line model in Figures 18 and 19. This log model produces large errors in both A and dA/dp throughout the domain used here. There is always too little absorption along paths between nearby layers, while there is usually too much absorption along paths between each level and space. Accurate values are found somewhere between these extreme paths. The nearby layer errors may result because this model relaxes to the "square root" limit $[A(p, p') \propto (\bar{p}\bar{m})^{1/2}]$ instead of the appropriate "linear" limit $[A(p, p') \propto \bar{m}]$, as $\bar{m} \rightarrow 0$. The functional form for this model also lacks an explicit Doppler or Voigt line-shape correction. This factor may account for the very large errors at low pressures.

Other errors produced by this simple empirical model may occur because it is being used to find the absorption along paths with pressures and absorber amounts outside the range of values used to fit the absorption coefficients. Our experience with logarithmic wideband models suggests that even when such models are good interpolation formulas, they should not be used to extrapolate. This problem cannot be avoided if only laboratory measurements of total absorption are used to fit the coefficients, since there are practical limits on the range of pressures and absorber path lengths that can be achieved in existing laboratory absorption cells. One can overcome this limitation by augmenting the existing laboratory measurements with reliable synthetic data generated by line-by-line models.

3.6. *The Integration Over Zenith Angle and the Diffusivity Factor*

To compute fluxes and heating rates in planetary atmospheres, point-to-point transmittances must be integrated over zenith angle to give the transmittance in flux form. This integration cannot be performed explicitly in most cases and must be approximated. In the results presented above, transmittances were evaluated along paths at four different zenith

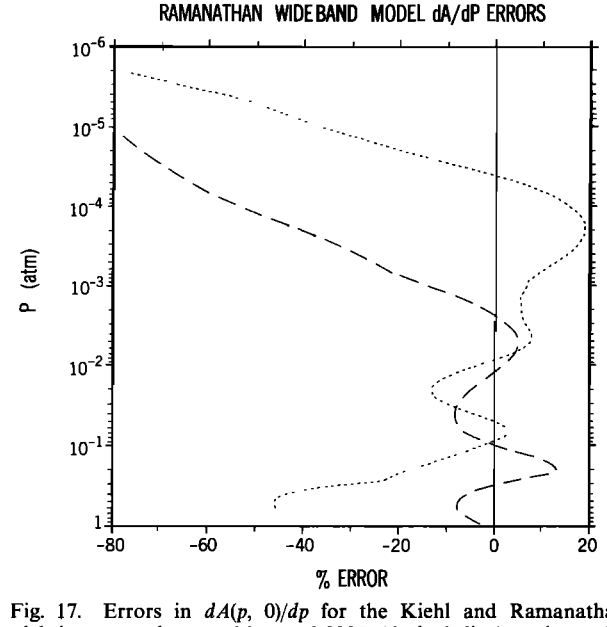

Fig. 17. Errors in $dA(p, 0)/dp$ for the Kiehl and Ramanathan model in atmospheres with $r = 0.0005$ (dashed line) and $r = 1.0$ (dotted line).

angles, and the integration was performed by Gaussian quadrature. The expense of these methods can therefore be reduced by up to a factor of 4 if the effect of this integration is parameterized by the *Elsasser* [1942] diffusivity approximation, which allows the transmittance to be evaluated in a single step. In this method the effect of the integration over zenith angle is approximated by multiplying the path-length-integrated absorber amount $\bar{m}$ by the diffusivity factor d. Elsasser shows that $d = 1.66$ is the best value for a regular model in the strong-line limit, and this value has been adopted by most investigators. *Rodgers and Walshaw* [1966] and *Armstrong* [1968, 1969] show that this approximation rarely produces absorption errors larger than 2% for optical paths in the terrestrial atmosphere. The effect of this approximation in a pure CO_2 atmosphere is not as well established, but an error analysis performed by *Armstrong* [1969] suggests that it may produce much larger errors (9%) for this case. We therefore tested the validity of this approximation for use in finding 15-μm transmittances for pure CO_2 atmospheres. The narrow-band Malkmus random model for the *Fels* [1979] approximate Voigt line shape was employed in these tests and a U.S. Standard Atmosphere Temperature profile was used. In the "standard" model the integration over zenith angle was performed numerically by four-point Gaussian quadrature. The "test" model used the diffusivity factor approximation instead. These models were used to find the absorption in ninety 5 cm^{-1} wide spectral intervals between 450 and 900 cm^{-1}. Results for each case were then summed to give the total broadband absorption along optical paths in a pure CO_2 model atmosphere.

We found that errors resulting from the diffusivity factor approximation for pure CO_2 atmospheres are only of the order of 2% and are therefore comparable to those reported by *Rodgers and Walshaw* [1966] for atmospheres with the terrestrial CO_2 mixing ratio. Most of this error occurs in the optically thin wings of the band. For example, in the spectral region 450–500 cm^{-1} the diffusivity factor model underestimates the absorption by as much as 15%. Fortunately, this spectral region accounts for only a small fraction (<3%) of the total band absorption.

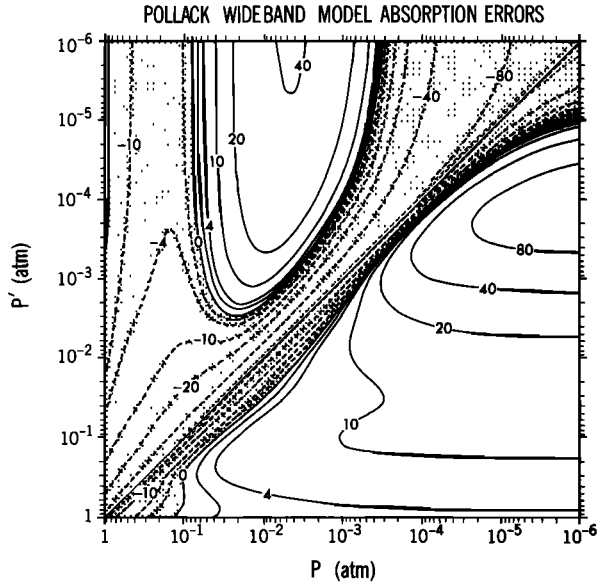

Fig. 18. Absorptance errors for the empirical wideband model described by *Pollack et al.* [1981] are shown for model atmospheres with CO_2 mixing ratios of 0.0005 (above $p = p'$ diagonal) and 1.0 (below $p = p'$ diagonal).

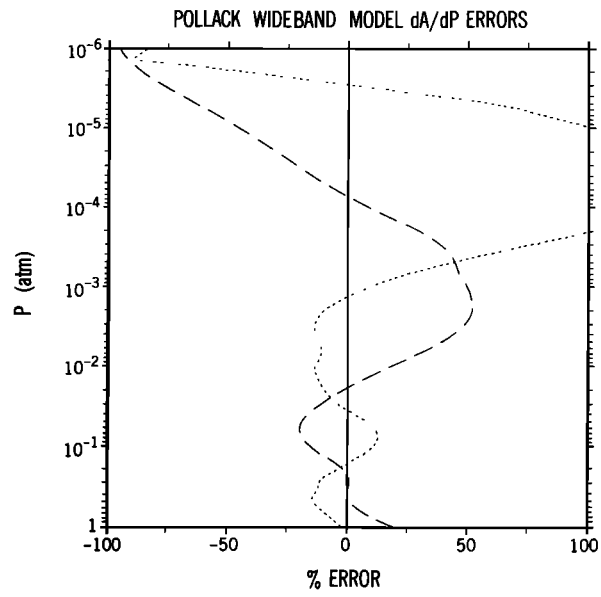

Fig. 19. Errors in $dA(p, 0)/dp$ for the *Pollack et al.* [1981] model in atmospheres with $r = 0.0005$ (dashed line) and $r = 1.0$ (dotted line).

SUMMARY AND CONCLUSIONS

We tested a hierarchy of approximate methods for finding transmittances in the CO_2 15-μm band. These methods can be divided into three classes. The first is composed of a series of narrow-band random models, including a general random model and models based on the *Malkmus* [1967] analytic line-strength distribution. These methods are versatile and much more efficient than the "exact" line-by-line model, but they still may be too expensive for use on some applications, since transmission must be evaluated in a large number of narrow spectral intervals if the total band-integrated transmittance is needed. The second class of models is represented by a new exponential wideband model. This model is neither a true "broadband" or "narrow-band" model, since it can be used to give the transmittance within a very broad section of the CO_2 15-μm band (as described here) or any small fraction of it in a single step. The third class of models includes the empirical logarithmic broadband models. These models provide the most efficient methods for finding 15-μm band transmittances. Our tests show that all three classes of models can produce accurate results for a wide range of optical paths, with pressures, temperatures, and CO_2 amounts like those encountered in the atmospheres of the terrestrial planets.

The physical band models, including the narrow-band random models and the exponential wideband model, are more reliable and versatile than the empirical broadband methods for the following reasons. First, these "band models" attempt to describe the structure and physical properties of the CO_2 15-μm band, instead of the shape of its "curve of growth." Hence if they accurately model the band's behavior for optical paths where measurements exist, they should provide a more reliable method for extrapolating beyond the range of existing absorption measurements. Second, these physical band models can be used to find the transmission within spectral intervals smaller than that occupied by the entire absorption band. This capability can be important in many atmospheric radiative transfer problems, including thermal flux and cooling rate calculations. In these problems the CO_2 transmittance must be spectrally convolved with the source function and with the transmittances of other gases

that absorb in the same spectral region. If only broadband transmittances are known, this convolution must be approximated by taking the product of the mean or spectrally integrated values of these quantities. This procedure can introduce an additional source of error if the transmission and source functions are spectrally correlated. For example, we have encountered relative flux errors ranging from 5 to 20% when broadband CO_2 15-μm transmittances were convolved with the mean Planck function for paths in an isothermal atmosphere at 250 K. Much larger errors have been found for nonisothermal paths.

In spite of these shortcomings, efficient broadband models are often the most appropriate tool for finding the CO_2 15-μm band transmittance in atmospheric radiative transfer problems. In fact, the convolution problems described above will not be the most significant source of error if (1) the source function varies slowly throughout the band, (2) CO_2 is the only important absorber in this spectral region, or (3) there are large uncertainties in the CO_2 absorber amounts or other atmospheric optical properties. Also, in problems where the CO_2 15-μm band is not the most important source of thermal opacity (such as in the terrestrial troposphere where H_2O absorption dominates), a somewhat less accurate treatment of CO_2 transmission is justified. Finally, broadband models often provide the only practical method for solving radiative transfer problems that require the transmittance to be computed many times. This factor alone will guarantee their popularity until computers are significantly more powerful and available than they now are.

Acknowledgments. We thank Jeff Kiehl for carefully reviewing the manuscript and offering many helpful suggestions. We also thank him for assisting us with the *Kiehl and Ramanathan* [1980] model. David Paige provided many helpful comments and tested the exponential broadband model in a Martian climate problem. His experience motivated improvements in the treatment of temperature dependence in this model. This work was supported in part by NSF grant ATM-7727262 and NASA grants NAGW-58 and NAGW-555. Contribution 4273 of the Division of Geological and Planetary Sciences, California Institute of Technology, Pasadena, California.

REFERENCES

Abramowitz, M., and I. A. Stegun (Eds.), Handbook of Mathematical Functions, *NBS Appl. Math. Ser., 55*, 1046, 1964.

Aoki, T., Semi-direct band models for the Transmittance calculation, *J Meteorol. Soc. Jpn., 56*, 112–119, 1978.

Armstrong, B. H., Theory of the diffusivity factor for atmospheric radiation, *J. Quant. Spectrosc. Radiat. Transfer, 8*, 1577–1599, 1968.

Armstrong, B H., The radiative diffusivity factor for the random Malkmus band, *J. Atmos. Sci., 26*, 741–743, 1969.

Bevington, P. R., *Data Reduction and Error Analysis for the Physical Sciences*, 336 pp., McGraw-Hill, New York, 1969.

Burch, D. E., D. Gryvnak, E. B. Singleton, W. L. France, and D. Williams, Infrared absorption by carbon dioxide, water vapor and minor atmospheric constituents, *Rep. AFCRL-62-698*, 316 pp., Air Force Cambridge Res Lab., Hanson Air Force Base, Bedford, Mass., 1962.

Cess, R. D., and V. Ramanathan, Radiative transfer in the atmosphere of Mars and that of Venus above the cloud deck, *J. Quant. Spectrosc. Radiat. Transfer, 12*, 933–945, 1972.

Cess, R. D., and S. N. Tiwari, Infrared radiative energy transfer in gases, *Adv. Heat Transfer, 8*, 229–283, 1972.

Drayson, S. R., Atmospheric transmission in the CO_2 bands between 12 μ and 18 μ, *Appl. Opt., 5*, 385–391, 1967.

Edwards, D. K., Absorption by infrared bands of carbon dioxide gas at elevated pressures and temperatures, *J. Opt. Soc. Am., 50*, 617–626, 1960.

Edwards, D. K., and A. Balakrishnan, Thermal radiation by combustion gases, *Int. J. Heat Mass Transfer, 16*, 25–40, 1973.

Edwards, D. K., and W. A. Menard, Comparison of models for correlation of total band absorption, *Appl. Opt., 3*, 621–625, 1964*a*.

Edwards, D. K., and W. A. Menard, Correlations for absorption by methane and carbon dioxide gases, *Appl. Opt., 3*, 847–852, 1964*b*.

Elsasser, W. M., *Heat Transfer by Infrared Radiation in the Atmosphere, Harvard Meteorol. Studies*, vol. 6, 107 pp., Harvard University Press, Cambridge, Mass., 1942.

Fels, S. B., Simple strategies for inclusion of Voigt effects in infrared cooling rate calculations, *Appl. Opt., 18*, 2634–2637, 1979.

Fels, S. B., and M. D. Schwarzkopf, An efficient, accurate algorithm for calculating CO_2 15-μm band cooling rates, *J. Geophys. Res., 86*, 1205–1232, 1981.

Goody, R. M., A statistical model for water vapor absorption, *Q. J. R. Meteorol. Soc., 78*, 165–169, 1952.

Goody, R. M., *Atmospheric Radiation*, vol. 1, *Theoretical Basis*, 436 pp., Oxford University Press, New York, 1964.

Goody, R. M., and M. J. S. Belton, Radiative relaxation times for Mars, a discussion of Martian atmospheric dynamics, *Planet Space Sci., 15*, 247–256, 1967.

Howard, J. N., D. L. Burch, and D. Williams, Near-infrared transmission through synthetic atmospheres, *J. Opt. Soc. Am., 46*, 186–190, 1956.

Hui, A. K., B. H. Armstrong, and A. A. Wray, Rapid computation of the Voigt and complex error functions, *Tech. Rep. G20-3357*, Palo Alto Sci. Cent., IBM Corp., Palo Alto, Calif., 1977.

Kasting, J. F., J. B. Pollack, and D. Crisp, The effects of high CO_2 levels on the surface temperature and oxidation state of the early Earth, *J. Atmos. Chem., 1*, 403–428, 1984.

Kiehl, J. T., and V. Ramanathan, CO_2 radiative parameterization used in climate models: Comparison with narrow band models and with laboratory data, *J. Geophys. Res., 88*, 5191–5202, 1983.

Kuo, H. L., Analytic infrared transmissivities of the atmosphere, *Contrib. Atmos. Phys., 50*, 331–349, 1977.

Malkmus, W., Random Lorentz band model with exponential-tailed S^{-1} line intensity distribution function, *J. Opt. Soc. Am., 57*, 323–329, 1967.

Pollack, J. B., C. Leovy, P. W. Greiman, and Y. Mintz, A Martian general circulation experiment with large topography, *J. Atmos. Sci., 38*, 3–29, 1981.

Ramanathan, V., Radiative transfer within the earth's troposphere and stratosphere: A simplified radiative-convective model, *J. Atmos. Sci., 33*, 1330–1346, 1976.

Ramanathan, V., and R. D. Cess, Radiative transfer within the mesospheres of Venus and Mars, *Astrophys. J., 188*, 407–416, 1974.

Ramanathan, V., and J. A. Coakley, Climate modeling through radiative-convective models, *J. Atmos. Sci., 16*, 465–489, 1978.

Rodgers, C. D., Some extensions and applications of the new random model for molecular band transmission, *Q. J. R. Meteorol. Soc., 94*, 99–102, 1968.

Rodgers, C. D., and C. D. Walshaw, The computation of infrared cooling rate in planetary atmospheres, *Q. J. R. Meteorol. Soc., 93*, 43–54, 1966.

Rodgers, C. D., and A. P. Williams, Integrated absorption of a spectral line with the Voigt profile, *J. Quant. Spectrosc. Radiat. Transfer, 14*, 319–323, 1974.

Rothman, L. and W. Benedict, IR energy levels and intensities of CO_2, *Appl. Opt., 17*, 2605–2611, 1978.

Wang, W. C., An analytical expression for the total band absorptance of infrared-radiating gases, *J. Quant. Spectrosc. Radiat. Transfer, 29*, 279–281, 1983.

D. Crisp, Division of Geological and Planetary Sciences, MS 107–25, California Institute of Technology, Pasadena, CA 91125.

S. B. Fels and M. D Schwarzkopf, Geophysical Fluid Dynamics Laboratory National Oceanic and Atmospheric Administration, Princeton University, Princeton, NJ 08542.

(Received October 5, 1985;
revised July 2, 1986;
accepted July 3, 1986.)